# Application of the Multifractal Spectrum to the Analysis of Vibration Signals Generated During Testing of Selected Composite Materials

Tomasz Figlus[1*], Mateusz Kozioł[2]

[1] Faculty of Transport and Aviation Engineering, Silesian University of Technology, Krasińskiego 8, 40-019 Katowice, Poland

[2] Faculty of Materials Engineering, Silesian University of Technology, Krasińskiego 8, 40-019 Katowice, Poland

* Corresponding author's e-mail: tomasz.figlus@polsl.pl

**ABSTRACT**

This paper presents a procedure for the application of a multifractal spectrum to analyse vibration signals obtained during static bending tests of selected fibre reinforced polymer matrix composite materials. The analyses were designed to determine the failure course of the composites tested under bending conditions. Non-stationary changes occurring in the signals include low- and high-energy symptoms of progressive damage in materials, which are difficult to identify and interpret, especially in the early stages. Determined using fractal leaders, the multifractal spectra of the vibration signals calculated for the different stages of the bending test allowed qualitative identification of the changes caused by progressive damage with different energy responses. In addition, the quantitative measures of change in the characteristics of the multifractal spectrum determined clearly indicated the changes occurring in the recorded signals. It can be concluded from the research that the proposed signal processing method based on a multifractal spectrum determined from non-stationary vibration signals is sensitive to changes occurring in these signals.

**Keywords:** vibration, multifractal spectrum, signal analysis, fibre reinforced polymer.

## INTRODUCTION

### Recording and analysis of vibroacoustic signals in materials testing

The recording of vibroacoustic signals and their analysis is often used to determine the vibroacoustic susceptibility of machinery and equipment [1–6] and to assess their technical condition [7–12]. Similarly, the analysis of acoustic emission signals and vibroacoustic signals recorded during the loading of components or structures can be used to assess events occurring inside materials during their straining [13–16]. These events are the local development of microcracks [17] or the fracture of individual fibres in composite materials [18]. From a signal analysis point of view, vibration and noise events can be quasi-stationary or dynamic, or a combination of both types. The waveform of the recorded signal is dependent on

factors such as time, amplitude and frequency of the forcing, load and others [7–12, 19–20]. Typical signal processing methods include computed point measures of time-domain signals, signal spectra in the frequency domain computed using the Fourier transform, or time-frequency distributions computed using the Gabor transform, the Wigner-Ville transform, or the wavelet transform. The choice of signal processing method and quantitative measures is very important from the point of view of inference in each specific case.

One of the more modern methods of analysing vibroacoustic signals is the use of fractals. Fractals are mathematical creations that are self-similar or infinitely complex and therefore have certain geometric shapes at any given scale. In the physical world, fractals have their prototypes in the form of curves and surfaces illustrating all cases of irregularity. From a mathematical point of view,

we can use fractals to describe various natural or technical phenomena, such as turbulence. The concept of fractal geometry can be found in paper [21]. The study [22] introduces a multifractal formalism based on wavelet leaders, which allows for a fractal spectrum over the entire range and its applicability to chirp or oscillating processes. A study of various multifractal phenomena in physics and chemistry was presented by the authors in [23]. In the study presented in [24], rolling bearings were diagnosed using multifractal features in combination with scaling exponents, multifractal spectrum and logarithmic cumulants. Combinations of the aforementioned features were assessed using a support vector machine (SVM). In [25], the authors used fractal methods to diagnose the technical condition of gear meshing based on the analysis of the recorded vibration acceleration signal. Studies using multifractal analysis was also presented in the paper [26], where this analysis was used to detect damage in building structures subjected to strong earthquakes. Another example of the application of fractal analyses is the study of radar signal interference presented in the paper [27]. These analyses showed a very high accuracy of the results obtained. The use of multifractal spectra for the detection of defects in composite materials was presented in paper [28]. The author of the study demonstrated that calculated spectra from acoustic signals can be related to the presence of defects or discontinuities in the materials analysed. The results of research work on the applicability of a multifractal spectrum to the assessment of tensile cracks in a polyvinylidene chloride/glass fiber composite are presented in paper [29]. In this study, the multifractal spectrum was found to be the result of changes in the mechanical properties present in the composite under study. In paper [30], a multifractal algorithm was used to describe the strength and plastic dependencies of the selected composites using generalized fractal pixel dimensions. A qualitative and quantitative description of structural materials using the multifractal spectrum was carried out in paper [31]. These studies have made it possible to assess the system properties of the structures and to characterize the self-organization in the materials analyzed. Research into the detection and quantification of damage to modern aircraft systems is presented in paper [32]. The authors used multifractals to assess dent-type damage. In view of the promising predictions of the application of fractal analysis in the study of materials, the authors have taken up this topic as part of this study. The study aims to assess the failure progression of several selected fiber reinforced polymer composite laminates, with particular emphasis on detecting the effects of failure at the early stage of the loading process. The signals were recorded during static bending tests of the composite samples. As a basis for the analysis, the authors propose the use of a multifractal spectrum based on wavelet leaders and its measures calculated from the recorded vibration signals of the composite samples. The main objective of the work is to present a new original methodology, including the method of bench testing and signal recording, the determination of the multifractal spectrum for the tests carried out, and relating these to the properties of the materials selected for testing. As part of the discussion of the analytical results obtained, the effectiveness of the methodology used in the analysis of material failure processes was assessed.

## Fiber reinforced polymer composite laminates

Fiber reinforced polymer (FRP) composite laminates are currently quite common materials for the vehicles and other transport constructions, valued especially for their low mass and high mechanical performance [33–36]. However, it took about 40 years for this group of materials to gain the trust of constructors, and one of the main doubts was the specific failure progress in these materials. FRP laminates are complex materials. To put it simply, they are composed of a polymer matrix and fibrous reinforcement. They present a complex model of destruction: hardly observable in the initial phase, violent-brittle in the main phase and remaining certain residual load capacity after the main destruction [37–39]. The process of fundamental destruction is preceded by initial damage, consisting in local cracking of individual fibres or small areas of the matrix [40], which cause invisible (but dangerous) damage of the material. The failure progress differs greatly for different types of laminates and depends on the fibre material, fibre form, fibre volume fraction and direction of fibre arrangement [41]. Hence, the long-term research process preceding the industrial implementation of laminates. As the study of the failure progress in laminates is an important element of their assessment, it is highly advisable practice to develop

new methodologies for such investigations. The methods used so far, using the analysis of the acoustic emission signal [13, 42] or the innovative approach of using the analysis of vibro-acoustic signals [14, 15], have produced very good results. The physical basis for the effectiveness of the use of acoustic and vibroacoustic methods in the failure analysis of laminates is the possibility of good separation of the signal from fibre cracking and matrix cracking. Large differences in the signal result from a large difference in the modulus of elasticity of these two components - even one hundred times [33]. The applied acoustic and vibroacoustic methods made it possible to analyse the course of damage also at the early stages of sample loading [19], which is extremely important when planning and predicting the applicability of the material.

New methods of analysing the signals obtained during the stressing of FRP laminates should focus on the initial area of the failure progress. The new fractal methodology allows - in a more comprehensive way - not only to detect, but also to categorise the effects of material destruction at individual stages. In this study selected materials are a tool for optimising the fractal method. After its adaptation the fractal method should become a modern and effective tool for evaluation of composite materials.

## MULTIFRACTAL WAVELET LEADER

### Multifractal wavelet leader - fundamental information

The analysis of signals using time-frequency methods such as wavelet transforms or Wigner-Ville transforms makes it possible to study local and fast-varying features present in signals. In some studies, the recorded signals are characterised by components that are difficult to interpret unambiguously, especially in the early stages of damage development. In these cases, new methods of processing and identifying the information components contained in the signals are sought for the evaluation of dynamic systems. One method that can be useful in these cases is multifractal methods based on wavelet leaders.

In multifractal analyses [23, 26, 27], by carrying out calculations using the discrete wavelet transform, we can derive the wavelet leaders $w(i,s)$ from the critically sampled coefficients.

For one-dimensional signals, the wavelet leaders are the supremes of the absolute values of the wavelet coefficients.

$$w(i,s) = sup_{s'<s} \left| \frac{1}{N_s} \int_{-\infty}^{\infty} f(t)\Psi\left(\frac{u-i'}{s'}\right) dt \right| \quad (1)$$

where:

$$\Psi_{s',i'}(t) = \Psi\left(\frac{u-i'}{s'}\right) \quad (2)$$

indicates a stretched and displaced wave form.

Based on the wave leaders, a scaling function is determined from the relationship:

$$S_w(q,s) = \left\{ \frac{1}{N_w} \sum_{i=1}^{N_w} \{w(i,s)\}^q \right\}^{\frac{1}{q}} \quad (3)$$

The location of the supremes themselves over time requires the calculation of wavelet coefficients. Hölder exponents $h$ are then determined from the supremes to determine local regularity, and the personality spectrum $F(h)$ is determined from the size of the set of Hölder exponents in the data.

$$h = \frac{d\tau(q)}{dq} \quad (4)$$

$$F(h) = inf_q(qh - \tau(q)) \quad (5)$$

As a result of the calculations, the resulting personality spectrum is used to evaluate the signals being analysed. For comparison purposes, spectrum characteristics such as its distribution, maximum and interval values, or other individually developed measures can be used for analysis. Examples of the signal measures determined in these cases can be consulted in the paper [22, 25, 26].

### Multifractal wavelet leader to vibration signal estimation

Given the potential of using the personality spectrum and Holder coefficients to assess qualitative and quantitative changes occurring in the signals, further research assumed that the following spectrum components and the measures calculated from them would be assessed:

- $c_p$ – is the value of the Holder index $h$ for which the value of the personality spectrum $F(h) = 1$,
- sum $h$ (6–11) – is the sum of the last 6 values of the Holder coeffficient $h$, which is expressed by the range $h \in \langle h_{max-6}, h_{max} \rangle$. This measure quantifies the change in selected values of the Holder coefficients of the personality spectrum, the significance of which was observed in the preliminary studies.

Figure 1 shows an example of a multifractal spectrum with the measures adopted for the study highlighted. In the study, it was assumed that the calculation of the multifractal spectrum values and Holder coefficients of the vibration signals would take place in 3 stages of composite bending test:

- range I – initial bending of the sample – where there are linear changes or the first quasilinear changes observed in the materials stress curve,
- range II – progressive bending of the sample – where there are quasilinear changes and the first non-linear changes observed in the materials stress curve,
- range III – advanced bending of the sample – where there are progressive non-linear changes observed in the stress curve in the materials up to the failure of the samples.

## TESTING AND THE SIGNAL RECORDING METHOD PROCEDURE

Static three-point bending tests were conducted on the INSTRON 4469 testing machine at state capacity of 5 kN (compression), which had been additionally equipped with a vibration measurement system [20]. The entire measuring device is shown in Figure 2.

The tests were conducted in accordance with the assumptions given in Table 1.

Relatively high speed (short test duration) allowed for acquisition of high-resolution data from vibroacoustic measurements. The initial analysis allowed the conclusion that the course of the characteristics of individual test pieces in both groups is very similar. In view of this, in order to
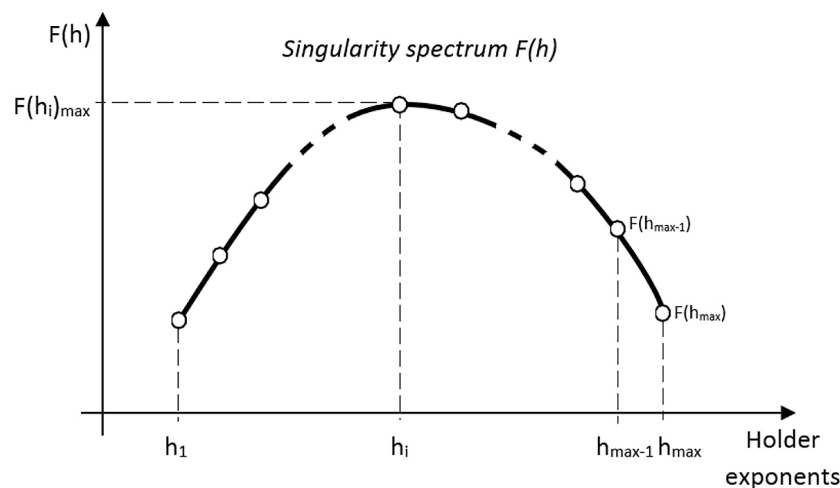


**Figure 1.** The singularity spectrum characteristic and representative parameters for calculating the spectrum
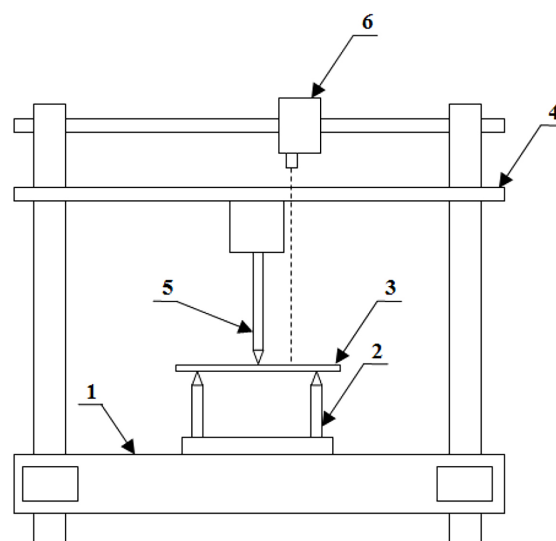


**Figure 2.** Measuring device diagram: 1 – device housing, 2 – supports, 3 – test piece, 4 – moveable traverse with force measuring head, 5 – load-imposing mandrel, 6 – laser vibrometer [20]

**Table 1.** Assumptions for bending tests

| Device | INSTRON 4369 universal testing machine (by Instron, USA) |
|---|---|
| Bending tests standard | PN-EN-ISO 14125/2001 [43] |
| Support spacing – specimen thickness constant ratio | 25/1 |
| Support spacing – glass fiber reinforced sepcimens | 50 mm |
| Support spacing – jute fiber reinforced sepcimens | 125 mm |
| Bending rate | 60 mm/min |
| Sampling frequency (for deflection and load) $f_{max}$ | 10 Hz |
| Specimen number for each group of materials | 5 |

achieve transparency of the presented argument, only 1 representative test piece from each group was selected for the vibration signal analysis. Test pieces in which the maximum stress was the closest to the average value for the given population were selected. The results of the tests were formerly applied in [14, 19]. Contactless measurements of the vibration velocity of composite specimens were performed using an OMETRON laser vibrometer. The laser beam is located in such a way that composite vibrations are measured halfway between the point where the test piece is initially supported and the point where the loading bar initially touches the piece. The vibration velocity of the test pieces were recorded at a sampling frequency of 20 kHz. The NI data acquisition card and LabView software was used to record the data while Matlab-Simulink software was used to process signals. Signal recording and tests were conducted until the test pieces clearly broke.

## RESEARCH MATERIALS

The vibroacoustic results obtained during three-point static bending tests of laminate samples were used to evaluate the fractal methodology. The tests were carried out on four types of samples made of laminates based on Epidian 53 epoxy resin cured with Z-1 hardener (manufacturer Organika Sarzyna, Poland), differing in the type of fibrous reinforcement:

1. Marked as "Composite I" - laminate reinforced with 6 layers of technical jute fabric with plain weave and areal mass of 350 g/m$^2$ – in total: 2100 g/m$^2$. Manufacturer: LENTEX, Poland.
2. Marked as "Composite II" - laminate reinforced with plain weave glass (E-glass) roving fabric, areal mass 350 g/m$^2$ - in total: 2100 g/m$^2$ (the same as the jute stack). Manufacturer: KROSGLASS, Poland.
3. Marked as "Composite III-W" - reinforced with glass (E-glass) 3D non-crimp fabric, areal mass of 3280 g/m$^2$, the samples cut and tested into warp direction. Manufacturer: 3TEX, USA.
4. Marked as "Composite III-P" - reinforced with glass (E-glass) 3D non-crimp fabric, areal mass of 3280 g/m$^2$, the samples cut and tested into weft direction. Manufacturer: 3TEX, USA.

The types of applied samples are imaged in Figures 3 and 4. The 3-point bending tests were performed with use of Instron 4469 testing machine in accordance with PN-EN ISO 14125 standard. The tested sample is illustrated in Figure 5.

Bending is quite characteristic type of loading for materials, it is complex in terms of stress (subsequent occurrence of stretching, pressing and
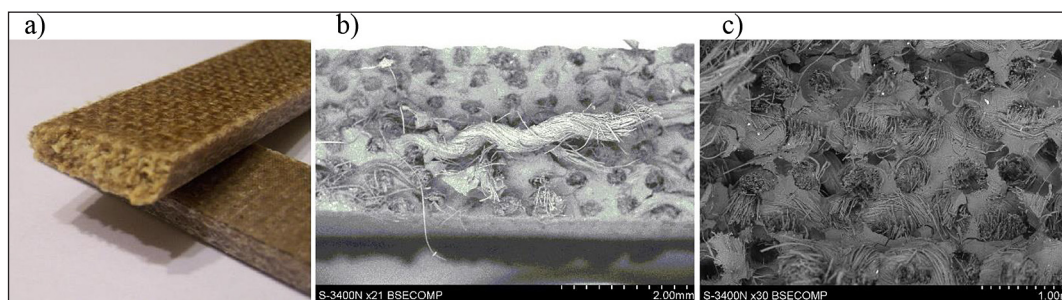


**Figure 3.** Samples tested – "Composite I": a) macro-scale view of the broken sample, b) and c) scanning electron microscope photo of the microstructure
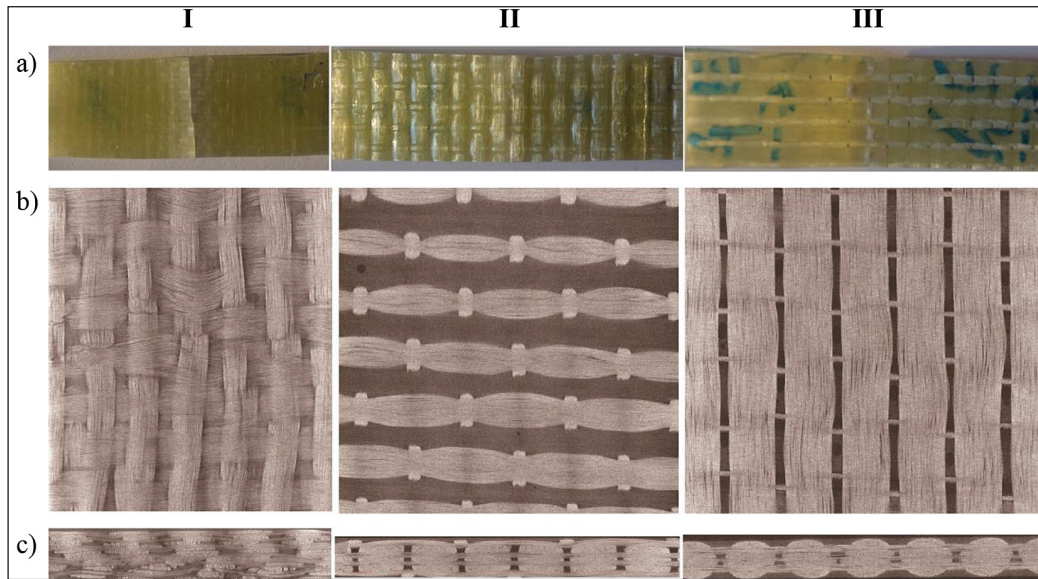
**Figure 4.** Samples tested: I – "Composite II", II - "Composite III-W", III - "Composite III-P":
a) macro-scale upper view of the sample, b) tomograph photo of the reinforcing structure – in-plane section,
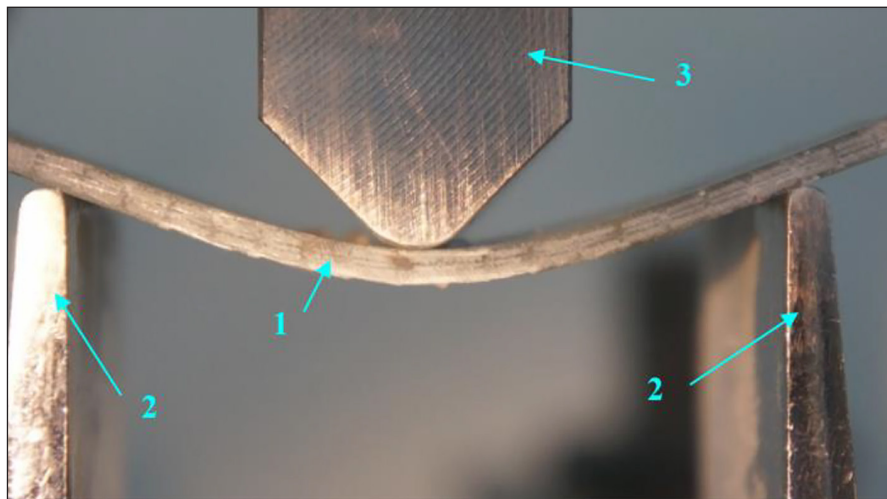c) tomograph photo of the reinforcing structure - cross section



**Figure 5.** 3-point static bending of a laminate sample: 1 – specimen, 2 – supports, 3 – loading bar

shearing in the sample). For the composite I (jute) we observe a typical rupture of the entire working section, probably started in the stretched part of the sample - it is visible in Figure 3a. The composite II (classic glass fibre reinforced polymer laminate) shows a very specific type of destruction – it starts in the pressed part of the sample and the main destruction effect is delamination of upper layers of the laminate [13]. One can see the specifically destructed sample in Figure 4a - only crack and whitened area of delamination, without complete decohesion. The composite III (W and P) breaks in 'between' the two above described. It shows some little delamination, but it mainly breaks after

breaking fibres in stretched part of the working section. The selected three types of samples are very good tools for evaluating the fractal method. They represent very similar type of structure, however, in case of composites II and III there is very big difference in elastic modulus between the components (glass – about 73 GPa, cured resin – about 2.5 GPa), but in case of composite I the elastic modulus of resin and the fibers is on equal. In addition, as was mentioned above, the composite II presents main destruction by delamination (matrix-oriented), but the composite III shows the destruction of the fibres (reinforcement-oriented). So, the method may be very widely tested on the applied set of samples.

## RESULTS AND DISCUSSION

In the first stage of the analyses, the recorded signals corresponding to the change in the stress state of the samples and the vibration velocity of the samples recorded at that time were identified. The results of these measurements are shown in Figures 6–9 indexed 'a'.

These studies show that progressive bending of the samples is accompanied by a change in stress in the test materials with characteristics varying from linear to non-linear (logarithmic). This process is initially accompanied by a small increase in vibration amplitude, which then increases significantly in terms of the non-linear change in the stress state of the materials.
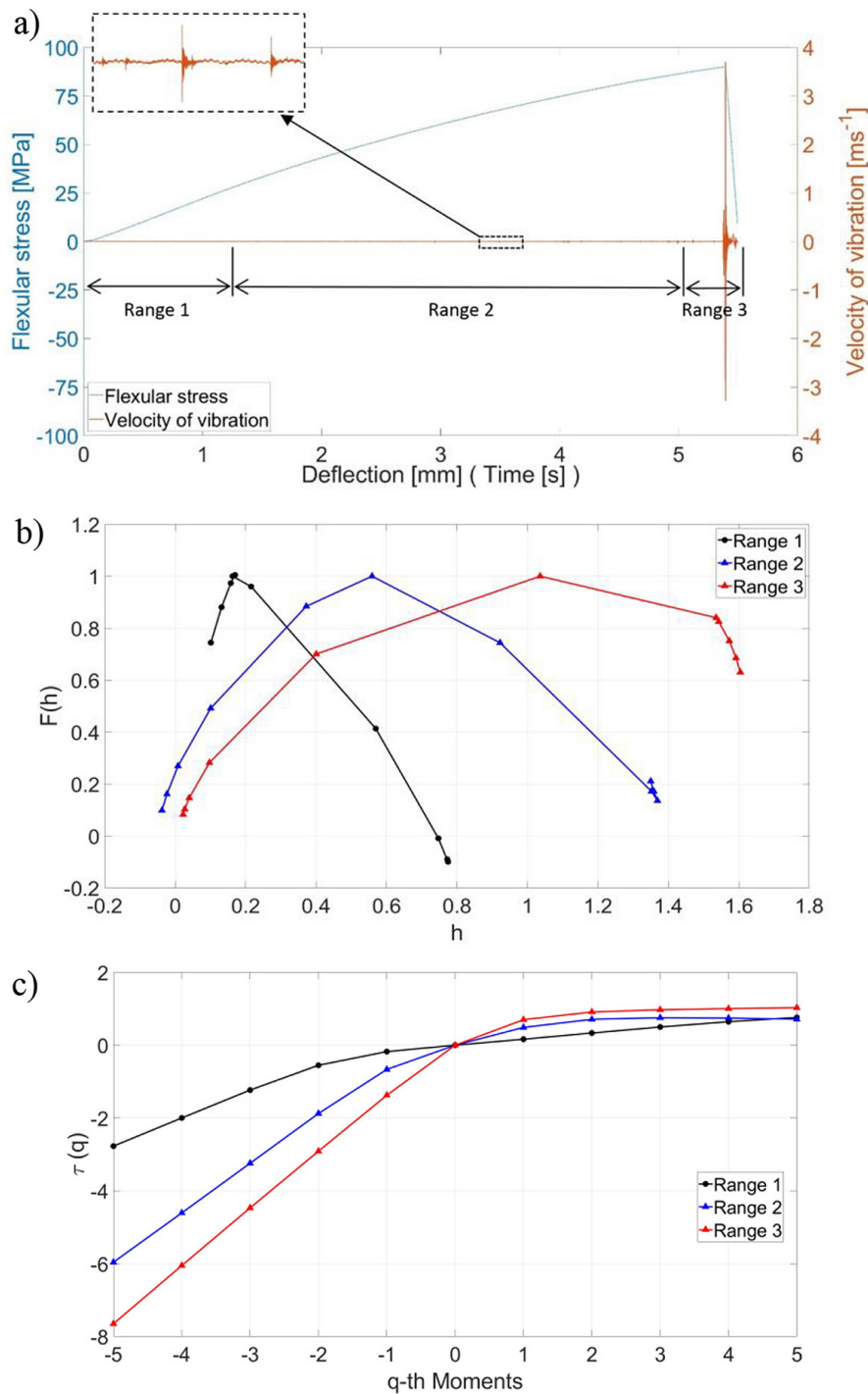


**Figure 6.** Measurement and analysis results for the Composite I sample (classic jute): a) Stress in the material and the course of the vibration velocity during the bending test, b) Multifractal Spectrum in the next ranges, c) Scaling exponents in the next ranges

**Figure 7.** Measurement and analysis results for the Composite II sample (classic glass): a) Stress in the material and the course of the vibration velocity during the bending test, b) Multifractal Spectrum in the next ranges, c) Scaling exponents in the next ranges
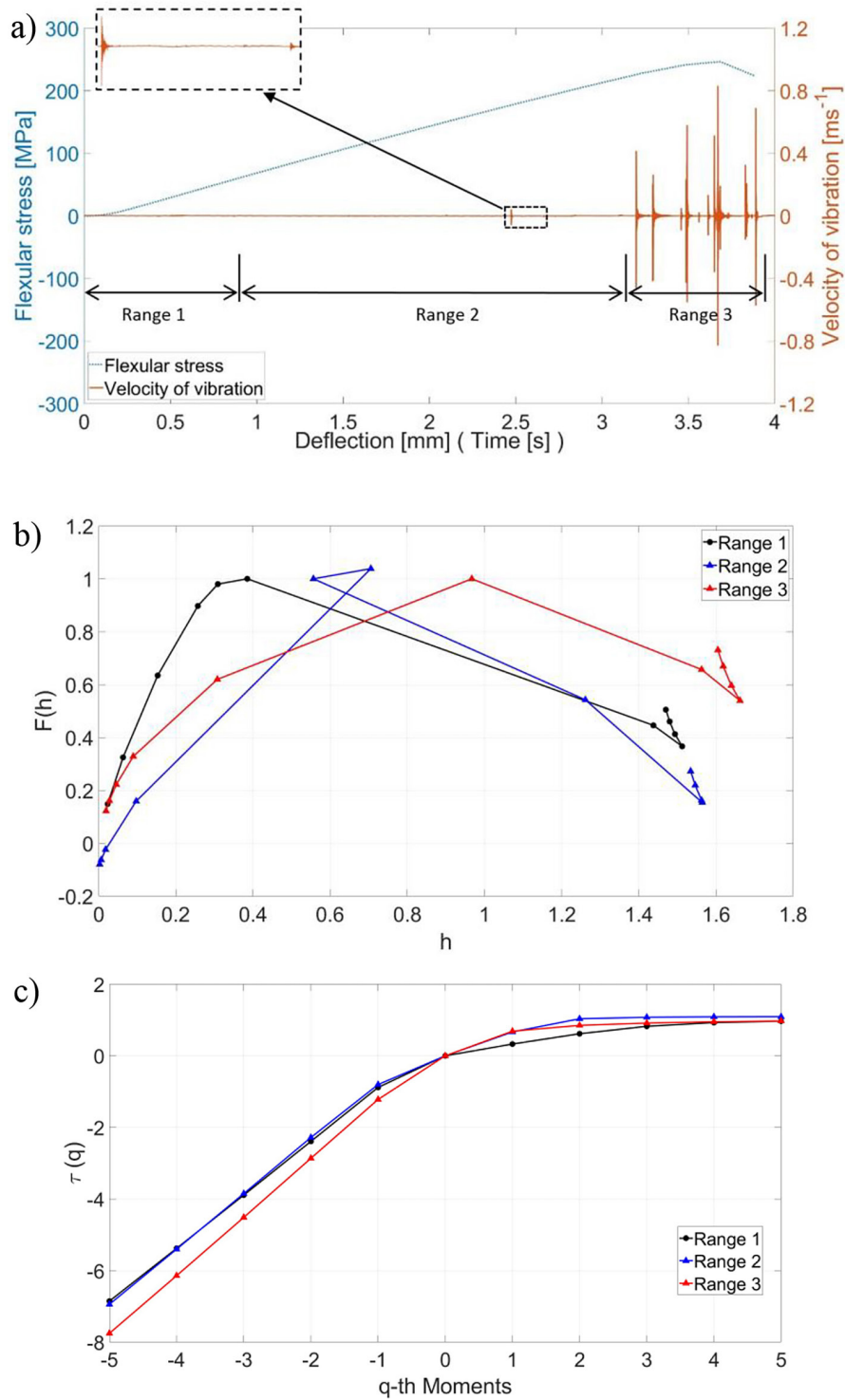
The change in vibration amplitude is different for the samples made of the materials tested, due to the different changes inducing internal degradation processes. An unambiguous and high-energy change in vibration amplitude that can be equated with significant internal damage in composite samples only occurs when the materials are significantly bent. These studies show that analysis of the raw vibration signal provides opportunities to assess direct damage to composite samples only to the extent of significant damage. Pre-existing changes in these
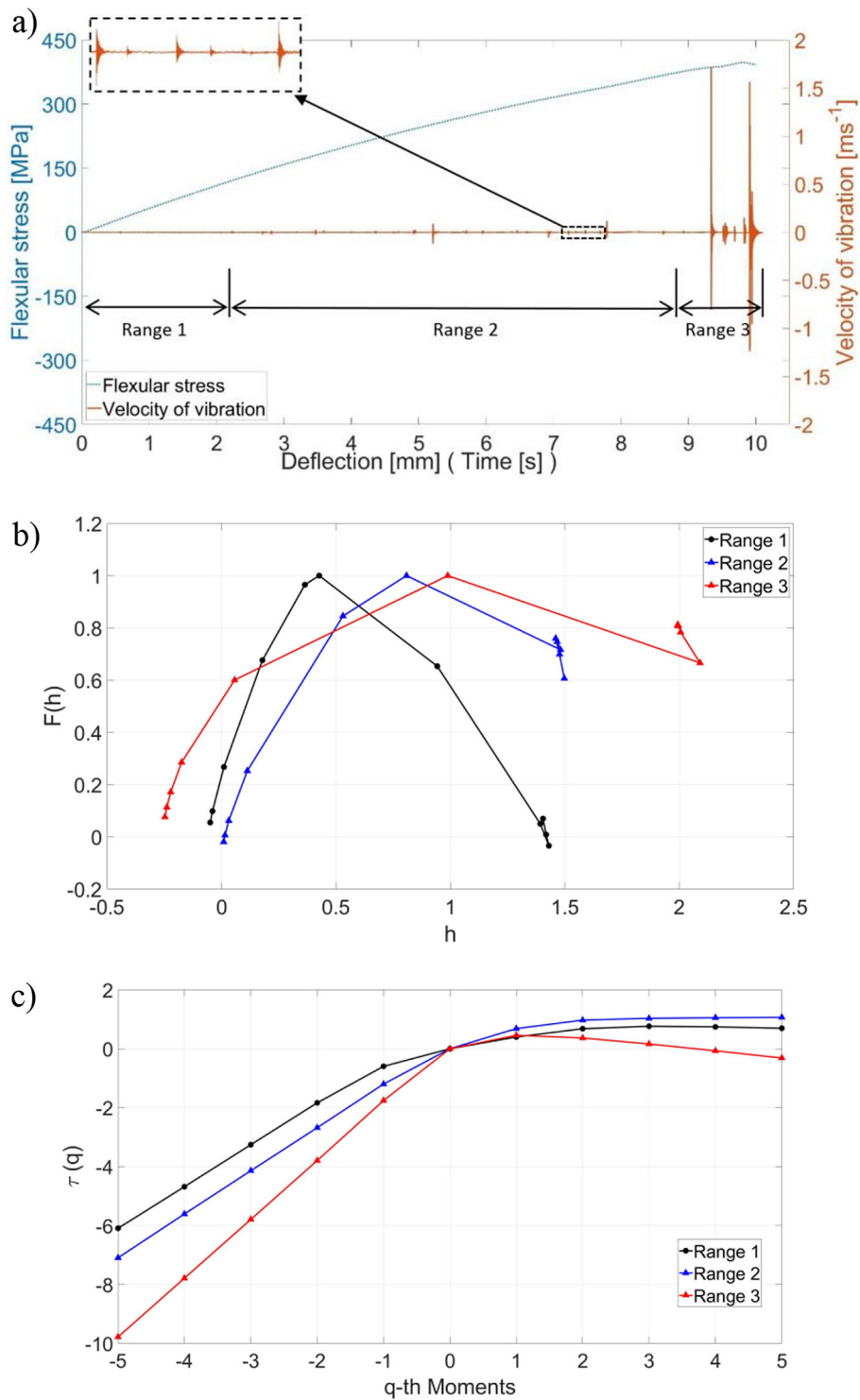
**Figure 8.** Measurement and analysis results for the Composite III-W sample (3D glass fibres arranged longitudinally): a) Stress in the material and the course of the vibration velocity during the bending test, b) Multifractal Spectrum in the next ranges, c) Scaling exponents in the next ranges

materials produce only low-level symptoms. In the next stage of the study, Holder coefficients, the corresponding multifractal spectra and scaling exponents in the I–III stages of the individual samples were calculated for the recorded vibration signals. In these studies, the possibility of early detection of state change symptoms in composite materials was assessed on the basis of vibration signal registration and its processing using the multifractal spectrum. The results of these calculations are shown in Figures 6–9 indexed 'b' and 'c'.
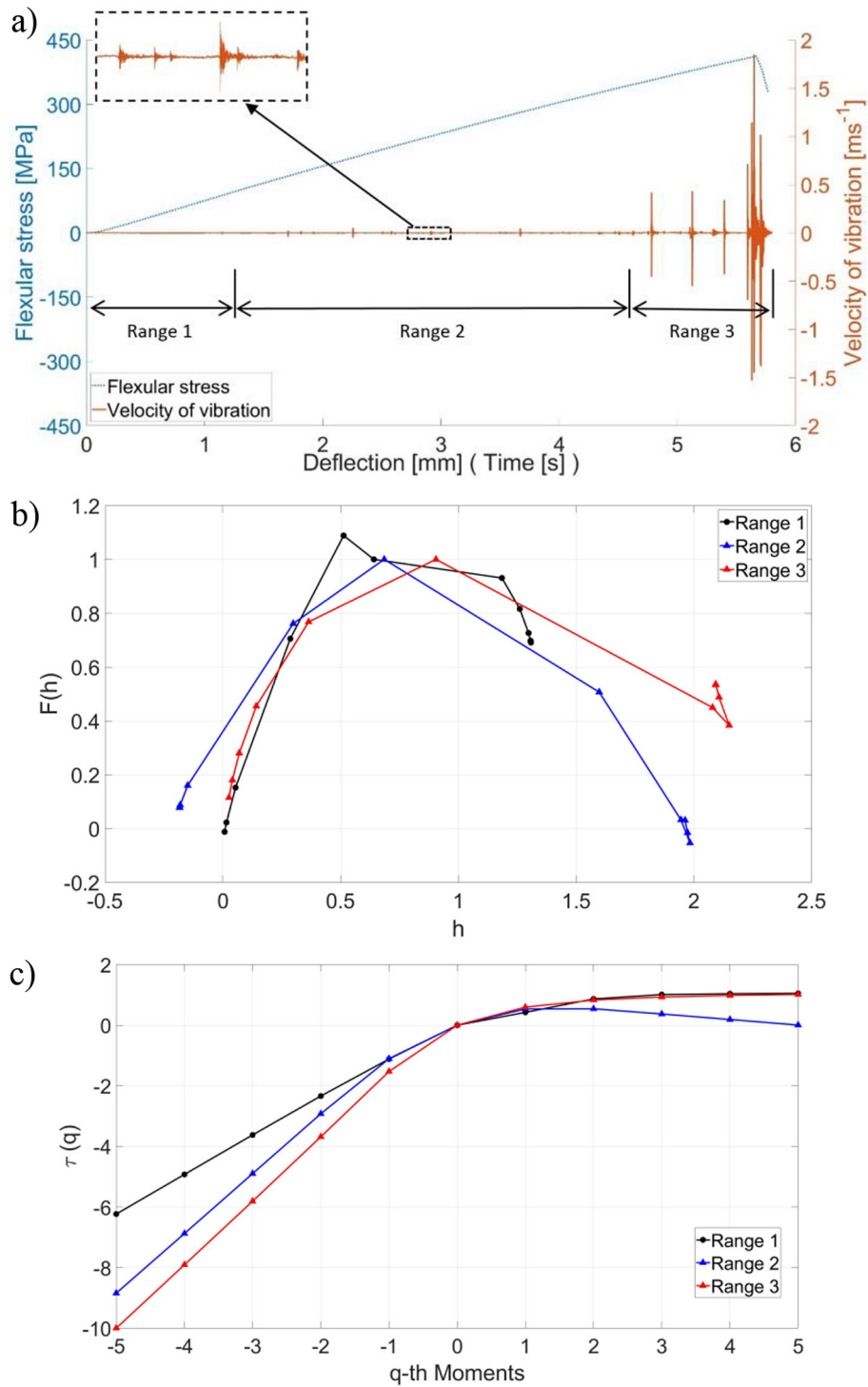
**Figure 9.** Measurement and analysis results for the Composite III-P sample (3D glass fibres arranged transversely): a) Stress in the material and the course of the vibration velocity during the bending test, b) Multifractal Spectrum in the next ranges, c) Scaling exponents in the next ranges

By dividing the recorded vibration signal into three stages relevant to the search for information about internal changes in the materials during the bending test, it was possible to calculate 3 successive sets of Holder coefficient values and personality spectra. The distributions in Figures 6–9 "b" enable an unambiguous qualitative identification of the results obtained, indicating that the values of the Holder coefficients increase with increasing bending of the samples, as well as the maximum value of the Holder coefficient corresponding to a multifractal spectrum value of 1. Adopting the

Holder coefficient and the personality spectrum calculated from vibration measurements of composite samples is therefore advisable for detecting small changes occurring in this type of composite. The results of the study showed that the shape of the personality spectrum broadens to the right as degradation of the composite samples progresses. The calculated Holder coefficients h take on values of increasing magnitude in successive calculation intervals.

In the next stage of the study, a quantitative evaluation of the changes observed in the multifractal distributions of the bending samples was carried out. The quantitative indices cp and Sum h (6–11) of the distributions were calculated according to the assumptions presented in Chapter 2.2, and the results are shown in Table 2–3 and Figure 10–11.

These studies show that the quantitative measures adopted from the multifractal spectrum are sensitive to the progressive changes in the composite materials during bending tests. Even slight damage occurring in the composite samples resulted in an increase in the values of the coefficients determined. The material that showed the greatest dynamics of change in the coefficients determined was the jute-reinforced composite. The cp index for this composite increased from the initial value of 0.1626 (no damage) to the value of 1.036 (significant damage), and the Sum h (6–11) coefficient increased from a value of 3.2415 (no damage) to a value of 8.8846 (significant damage). For the other samples, the 3D glass fabric-reinforced composite when positioned transverse to the main loading direction showed a good dynamic change in measure, with the cp coefficient increasing from 0.6415 (no damage) to 0.9051 (significant damage) and the Sum h (6–11) coefficient increasing from 7.0009 (no damage) to 11.4277 (significant damage). The observed increases do not vary significantly, but allow some trends to

**Table 2.** The cp index for the subsequent tested deflection ranges of samples from Composite I, II, III-W, III-P

| Range | cp [ - ] | | | |
|---|---|---|---|---|
| | Composite I | Composite II | Composite III-W | Composite III-P |
| Range 1 | 0.1626 | 0.3851 | 0.4267 | 0.6415 |
| Range 2 | 0.5588 | 0.5566 | 0.8084 | 0.6854 |
| Range 3 | 1.036 | 0.967 | 0.9885 | 0.9051 |

**Table 3.** The Sum h (6–11) coefficient for subsequent tested deflection ranges of Composite I, II, III-W, III-P samples

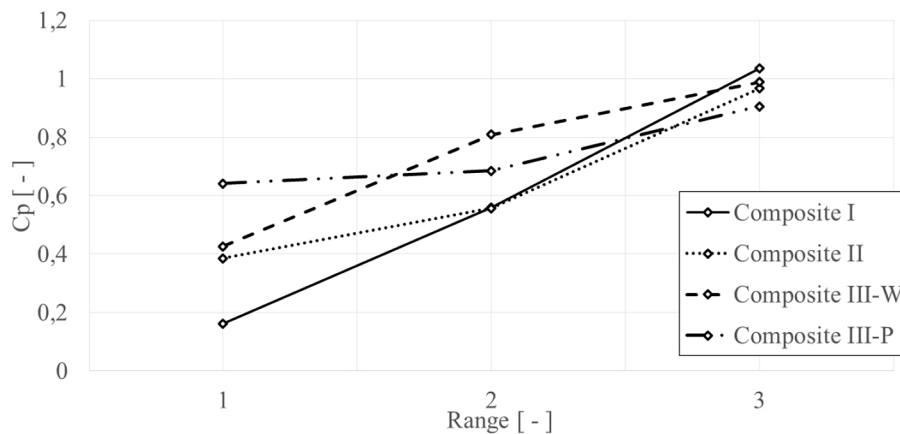| Range | Sum h (6–11) [–] | | | |
|---|---|---|---|---|
| | Composite I | Composite II | Composite III-W | Composite III-P |
| Range 1 | 3.2415 | 7.7783 | 7.016 | 7.0009 |
| Range 2 | 6.9114 | 8.0251 | 8.1913 | 10.1483 |
| Range 3 | 8.8846 | 9.0551 | 11.0691 | 11.4277 |



**Figure 10.** Variation in cp coefficient for subsequent tested deflection ranges of samples made from Composite I, II, III-W, III-P
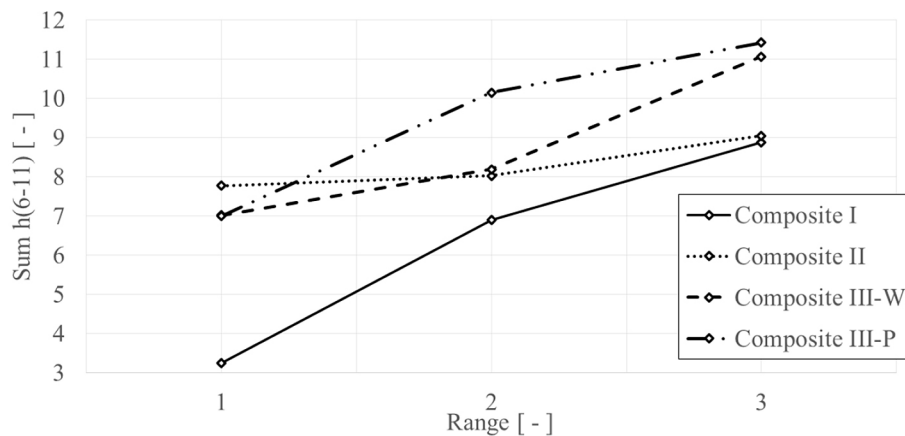
**Figure 11.** Variation of the sum h (6–11) coefficient for the subsequent tested deflection ranges of samples made of Composite I, II, III-W, III-P materials

be determined for the different types of composites. In a 3D glass fabric-reinforced composite, we are dealing with a well-organised structure that is reproducible throughout the volume. The onset of failure during bending of a beam made of this type of composite consists of the fracture of small strands of glass fibres with a relatively high elastic modulus (73 GPa) in the tensile part of the beam. A high rupture modulus is associated with a correspondingly high energy released during decohesion, which in turn translates into a higher energy of disruption of the continuum surrounding the site of this event. The main deterioration of the 3D glass fabric-reinforced composite also mainly involves mass fracture of the fibre strands. So, both the first observed failure effects and the fundamental failure of the composite involves elastic events of relatively high energy, so the difference between the observed parameter magnitudes is going to be smaller than for less well organised composite structures. For example, for a composite reinforced with jute fibres, the difference in fibre and matrix modulus is small. In addition, due to the peculiar multi-level structure of the jute fibres, there are the effects of their strain, which (in contrast to the well-ordered glass fibres in 3D fabric) takes place over a rather large strain range. In view of the above, the failure mechanics of jute-reinforced composites rather start with matrix fracture and the essential failure, however, is mainly related to the fracture of the tensile fibres. Despite their relatively low elastic modulus (<10 GPa), the failure progression from initial fracture to primary failure is characterised by a more variable energy than that of 3D glass

reinforcement. Hence the greater variation in recorded fractal parameters.

The calculated measures for classic glass and 3D glass with longitudinally arranged fibres were also characterised by an increase in value with progressive damage, but the dynamics of the change in measures was slightly lower.

Studies have shown that by using signal processing with multifractal spectra, it is possible to detect the first slight damage in composite samples, which are typically characterised by low-energy symptoms of change. Symptoms of this damage were not previously observable in the material's stress waveforms, as the destructive nature of the progressive changes did not clearly affect the change in the stress curve from linear to nonlinear characteristics. The results obtained extend the applicability of vibroacoustic signals in monitoring early changes occurring in composite samples presented by the authors in papers [44–45].

## CONCLUSIONS

Analysis of the vibration signal obtained during static bending of FRP composite beams using multifractal spectra developed on the basis of wavelet leaders has proved to be an effective tool for assessing the failure progression of the tested materials. The most important observations made during the implementation of the study are as follows:
- The results of vibration measurements during bending tests are characterised by numerous information contents with low-energy non-stationary components that are difficult to

interpret directly. However, such signals can be the first signs of damage and are therefore valuable from the diagnostic point of view. Of the test methods used to date, multifractal analysis has identified moments at which low-energy events were most likely to be associated with structural damage. Previously used methods were unable to extract them from the noise. Positive results were obtained for all four composites tested.

- The vibration signal of the composite samples recorded during the bending test also contains high-energy non-stationary changes that are difficult to identify. The use of multifractal signal processing enabled the identification of material failure symptoms occurring during the initial bending period of the samples, associating them mainly with high-modulus fibre failure and allowing these events to be filtered out of the noise.

- The research carried out clearly indicates that signal processing methods based on multifractal spectra can be useful for processing vibration signals when identifying early damage in FRP composite materials.

## REFERENCES

1. Kuczaj M., Wieczorek A.N., Konieczny Ł., Burdzik R., Wojnar G., Filipowicz K., Głuszek G. Research on vibroactivity of toothed gears with highly flexible metal clutch under variable load conditions. Sensors 2023, 23, 287. https://doi.org/10.3390/s23010287

2. Yang C., Zhang L., Han Y., Cai D., Wei S. Study on the transmission and evolution characteristics of vibration wave from vibratory roller to filling materials based on the field test. Appl. Sci. 2020, 10, 2008. https://doi.org/10.3390/app10062008

3. Jírová R., Pešík L. Pneumatic vibroisolation system of the base desk with natural frequency regulation. Scientific Journal of Silesian University of Technology. Series Transport. 2021, 113, 91–100. https://doi.org/10.20858/sjsutst.2021.113.7

4. Figlus T., Kozioł M., Kuczyński Ł. Impact of application of selected composite materials on the weight and vibroactivity of the upper gearbox housing. Materials, 2019, 12(16), 2517. https://doi.org/10.3390/ma12162517

5. Figlus T., Kozioł M., Kuczyński L. The effect of selected operational factors on the vibroactivity of upper gearbox housings made of composite materials. Sensors (Switzerland), 2019, 19(19), 4240. https://doi.org/10.3390/s1919424

6. Isaac C.W., Wrona S., Pawelczyk M., Karimi H.R. Modelling vibro–acoustic response of lightweight square aluminium panel influenced by sound source locations for active control. Sci Rep, 2022, 12, 10727. https://doi.org/10.1038/s41598-022-14951-y

7. Tong Q., Liu Z., Lu F., Feng, Z., Wan, Q. A New de-noising method based on enhanced time-frequency manifold and kurtosis-wavelet dictionary for rolling bearing fault vibration signal. Sensors 2022, 22, 6108. https://doi.org/10.3390/s22166108

8. Teng Z., Teng S., Zhang J., Chen G., Cui F. Structural damage detection based on real-time vibration signal and convolutional neural network. Appl. Sci. 2020, 10, 4720. https://doi.org/10.3390/app10144720

9. Waszczuk-Młyńska A., Gałęzia A., Radkowski S. Fault identification in membrane structures using the hilbert transforms. Sensors 2022, 22, 6224. https://doi.org/10.3390/s22166224

10. Perez-Sanjines F., Peeters C., Verstraeten T., Antoni J., Nowe A., Helsen, J. Fleet-based early fault detection of wind turbine gearboxes using-informed based on coherence. Mechanical Systems and Signal Processing, 15 February 2023, 185, 109760. https://doi.org/10.1016/j.ymssp.2022.109760

11. Kuzio D., Zimroz R., Wyłomańska A., Identification of fault frequency variation in the envelope spectrum in the vibration-based local damage detection in possible changing load/speed conditions. Measurement, 15 August 2023, 218, 113148, https://doi.org/10.1016/j.measurement.2023.113148

12. Czech P. Diagnosing faults in the timing system of a passenger car spark ignition engine using the Bayes classifier and entropy of vibration signals. Scientific Journal of Silesian University of Technology. Series Transport. 2022, 116, 83–98. https://doi.org/10.20858/sjsutst.2022.116.5

13. Kozioł M., Śleziona J. Przebieg zniszczenia przy statycznym zginaniu laminatów poliestrowo – szklanych o wzmocnieniu zszywanym, Polimery, 2008, 53, 11–12, 876–882.

14. Figlus T., Kozioł M. Evaluation of failure progress in glass- and jute-fibre reinforced polymer laminates by analysis of vibration and noise, Journal of Vibroengineering, 2014, 7, 3449–3468.

15. Koziol M., Figlus T. Failure progress of 3D reinforced GFRP laminate during static bending, Evaluated by Means of Acoustic Emission and Vibrations Analysis, Materials, 2015, 8(12), 8751–8767, https://doi.org/10.3390/ma8125490

16. Decker Ž., Rudzinskas V., Drozd K., Caban J., Tretjakovas J., Nieoczym A., Matijošius J., Analysis of the vehicle chassis axle fractures. Materials, 2023, 16(2), 806. https://doi.org/10.3390/ma16020806

17. Katoh M., Nishio K., Yamaguchi T., Mukae S. Microcracks in aluminium alloys developed in the cleaning

action region. Welding International, 1995, 95, 360–365, https://doi.org/10.1080/09507119509548814

18. Sharifpour F., Montesano J., Talreja R. Micromechanical assessment of local failure mechanisms and early-stage ply crack formation in cross-ply laminates. Composites Science and Technology, 2022, 220, 109286, https://doi.org/10.1016/j.compscitech.2022.109286

19. Figlus T., Kozioł M. Diagnosis of early-stage damage to polymer - glass fibre composites using non-contact measurement of vibration signals, Journal of Mechanical Science and Technology, 2016, 308, 3567–3576, https://doi.org/10.1007/s12206-016-0717-1

20. Figlus T., Koziol M. Method for evaluating destruction of composite materials, involves measuring instantaneous sound pressure level in vicinity of sample located at supports of body in direction perpendicular or parallel to axis of movement of mandrel, Patent Number: PL406442-A1, PL226933-B1.

21. Mandelbrot BB. The fractal geometry of nature. San Francisco: W.H. Freemann and Co.; 1982.

22. Lashermes B., Jaffard S., Abry P. Wavelet leader based multifractal analysis. Conference Paper in Acoustics, Speech, and Signal Processing, 1988. ICASSP-88., 1988 International Conference on April 2005. https://doi.org/10.1109/ICASSP.2005.1415970

23. Stanley HE, Meakin P. Multifractal phenomena in physics and chemistry. Nature 1988, 335, 405–9.

24. Du W., Tao J., Li Y., Liu Ch. Wavelet leaders multifractal features based fault diagnosis of rotating mechanism, Mechanical Systems and Signal Processing, 2014, 43(1–2), 57–75, https://doi.org/10.1016/j.ymssp.2013.09.003

25. Puchalski A., Komorska I. Data-driven monitoring of the gearbox using multifractal analysis and machine learning methods. MATEC Web Conf., 2019, 252, 06006, https://doi.org/10.1051/matecconf/201925206006

26. Pnevmatikos N., Konstandakopoulou F., Blachowski B., Papavasileiou G., Broukos P., Multifractal analysis and wavelet leaders for structural damage detection of structures subjected to earthquake excitation, Soil Dynamics and Earthquake Engineering, 2020, 139, 106328, https://doi.org/10.1016/j.soildyn.2020.106328

27. Xi C., Zhang S., Xiong G., Zhao H., Multifractal analysis of sea clutter and target detection based on the Wavelet Leaders method, 2016 IEEE International Conference on Digital Signal Processing (DSP), Beijing, China, 2016, 652–656, https://doi.org/10.1109/ICDSP.2016.7868639

28. Akhmetkhanov R.S. Application of fractal theory in diagnostics of composite materials, IOP Conference Series: Materials Science and Engineering Open Access, January 2021, 1023(113), 012002, https://doi.org/10.1088/1757-899X/1023/1/012002

29. Zhang Y.-H., Bai B.-F., Li J.-Q., Chen J.-B., Shen C.-Y. Multifractal analysis of the tensile fracture morphology of polyvinylidene chloride/glass fiber composite, Applied Surface Science, 257(7), 2984–2989, https://doi.org/10.1016/j.apsusc.2010.10.104

30. Meshalkin V.P., Butusov O.B., Reverberi A., Kolmakov A.G., Sevostyanov M.A., Garabadzhiu, A.V., Alexandrova A.G. Multifractal Analysis of the Mechanical PropOKerties of the Texture of Biopolymer-Inorganic Composites of Chitosan-Silicon Dioxide, Energies, 2022, 15, 7147, doi.org/10.3390/en15197147

31. Kheifetz M.L., Senyut V.T., Kolmakov A.G., Bazrov B.M., Klimenko S.A., Kopeikina M. Yu. Application of Multifractal Analysis for Research of Structural Materials, Nonlinear Phenomena in Complex Systems, 2021, 24(4), 338–347, https://doi.org/10.33581/1561-4085-2021-24-4-338-347

32. Agastinose Ronickom J.F., Retnakaran Sobhana A., Robert F., Nadaradjane S.M.R., Chelliah S.K. Automated damage detection and characterization of polymer composite images using Tsallis-particle swarm optimization-based multilevel threshold and multifractals, Polymer Composites, 41(8), 3194–3207, https://doi.org/10.1002/pc.25611

33. Boczkowska A., Krzesiński G. Kompozyty i techniki ich wytwarzania. Wydawnictwo OWPW, Warszawa, 2016.

34. Aly N.M. A review on utilization of textile composites in transportation towards sustainability. IOP Conference Series: Materials Science and Engineering, 2017, 254, 4, https://doi.org/10.1088/1757-899X/254/4/042002

35. Zurowski W., Zepchlo J., Cep R., Cepova L., Rucki M., Krzysiak Z., Caban J., Samociuk, W. The effect of powder and emulsion binders on the tribological properties of particulate filled glass fiber reinforced polymer composites. Polymers, 2023, 15(1), 245, https://doi.org/10.3390/polym15010245

36. Walczak M., Szala M., Pieniak D. Effect of water absorption on tribological properties of thermoplastics matrix composites reinforced with glass fibres. Advances in Science and Technology Research Journal, 2022, 16(2), 232–239, https://doi.org/10.12913/22998624/147515

37. Katunin A., Pawlak S., Wronkowicz-Katunin A., Tutajewicz D. Damage progression in fibre reinforced polymer composites subjected to low-velocity repeated impact loading. Composite Structures, 2020, 252, 112735, https://doi.org/10.1016/j.compstruct.2020.112735

38. Zhang A., Zhang D., Lu H. Residual bending strength after impact of CFRP laminates in hygrothermal condition. Journal of Composite

Materials, 2013, 47, 28, 3535–3542, https://doi.org/10.1177/0021998312467384

39. Kozioł M., Rutecka M., Śleziona J. Ocena wytrzymałości resztkowej zszywanych laminatów żywica poliestrowa – włókno szklane, Kompozyty, 2006, 62, 3–7.

40. Okabe T., Imamura H., Sato Y., Higuchi R., Koyanagi J., Talreja R. Experimental and numerical studies of initial cracking in CFRP cross-ply laminates. Composites Part A, 2015, 68, 81–89, https://doi.org/10.1016/j.compositesa.2014.09.020

41. Saito H., Morita M., Kawabe K., Kanesaki M., Takeuchi H., Tanaka M., Kimpara I. Effect of ply-thickness on impact damage morphology in CFRP laminates. Journal of Reinforced Plastics and Composites, 2011, 30(13), 1097–1106, https://doi.org/10.1177/0731684411416532

42. Saeedifar M., Zarouchas D. Damage characterization of laminated composites using acoustic emission: A review. Composites Part B, 2020, 195, 108039, https://doi.org/10.1016/j.compositesb.2020.108039

43. Polish Committee for Standardization. Fibre-Reinforced Plastic Composites – Determination of Flexural Properties; PN-EN-ISO 14125: 2001; Polish Committee for Standardization: Warsaw, Poland, 2001.

44. Craddock J.N.: Behavior of composite laminates after first-ply-failure. Composite Structures, 1985, 3(2), 187–200, https://doi.org/10.1016/0263-8223(85)90043-1

45. Zhu M., Chen D., Hu Q. Failure mechanisms and reinforcing modes of ply splice fiber-reinforced composite laminates under tensile load. Materials, 2019, 12(18), 2912, https://doi.org/10.3390/ma12182912